Kalpa Publications in Computing
Volume 19, 2024, Pages 277–287
Proceedings of 6th International Conference
on Smart Systems and Inventive Technology

Ultrawideband Microstrip Antenna for Wireless Body Area Network in IOT Applications

Susmitha Krishna G[1], Alekhya Bandi[1], Poojitha N[1] and SreePranavi Polani[1]
[1] V R Siddhartha Engineering College, BZA, India.
susmithachowdary1302@gmail.com, alekhya@vrsiddhartha.ac.in,
poojithanakkala@gmail.com, pranavipolani@gmail.com

Abstract

Creating a microstrip antenna for Wireless Body Area Network (WBAN) applications is a major challenge in the Internet of Things (IoT). Sports monitoring, healthcare, and other industries are among the areas for which this antenna is intended for usage. It operates in the 9.4 to 18.3 GHz UWB frequency range. It follows a meticulous modelling and design process. To miniaturize without compromising performance, the goal is to employ cutting- edge techniques like compact architectures and fractal geometries. In order to provide dependable connectivity in body-centric Internet of Things applications, the antenna aims to demonstrate perfect impedance matching and an omnidirectional radiation pattern.

Keywords: Wireless Body Area Network (WBAN), Internet of Things (IoT), impedance matching, omnidirectional radiation pattern.

1 Introduction

The many benefits of wearable and portable technology, including its ability to function as a personal digital assistant and offer internet access and multimedia services, have drawn a great deal of research in recent years. Examples of wearable technology that are currently the subject of extensive research are smart watches and rings. These smart gadgets have several sensors installed in them, which enables wireless communication between them and other gadgets, like smartphones. Over the past ten years, flexible and textile-based electronics have gained attention because of their many possible uses in the future, such as wireless tracking, public safety, health monitoring, and other areas.

Smart watches and rings have emerged as prominent examples, garnering significant attention in research. These devices are equipped with multiple sensors, facilitating wireless communication with smartphones and other gadgets. The versatility of wearable tech extends to various applications, including wireless tracking, public safety, and health monitoring, prompting a surge of interest in flexible and textile-based electronics over the past decade [1]. One study proposes the use of

monopole elements positioned 4 mm apart to construct a tri-band Multiple-Input Multiple-Output (MIMO) antenna system, demonstrating good isolation. Incorporating neutralization lines in a symmetrical configuration enhances isolation, resulting in quasi-omnidirectional radiation patterns and a low envelope correlation coefficient suitable for portable MIMO applications [2]. Another study introduces a compact eight-element H-shaped dual-band MIMO antenna system integrated into the side edge frame of sub-6 GHz 5G handsets. This design effectively minimizes mutual interaction among the four radiating elements on each side, enabling operation in two distinct frequency bands within the designated 5G spectrum [3].

A boat-shaped multi-band MIMO antenna tailored for 5G/W LAN applications tackles mutual coupling issues by leveraging split ring resonators, stubs, and a faulty ground construction. Operating at 2.32 GHz and 5.2 GHz, it achieves increased isolation and dual-band functionality, covering a bandwidth obstruction from 2.22 to 2.42 GHz and 5.142 to 5.706 GHz [4]. A groundbreaking advancement in wireless communication is embodied in a two-port full-duplex microstrip patch antenna system. This milestone surpasses conventional barriers, significantly reducing interference and ensuring robust signal integrity without the need for additional circuitry. The antenna's innovative design, incorporating defective ground and near-field decoupling structures, achieves extraordinary mutual coupling reduction, below -90 dB, simplifying construction and enhancing overall performance [5]. Wearable technology sees a notable stride with the development of a flexible two - element dual-band MIMO antenna utilizing conductive fabric, MKKTN260. This high isolation mitigates interference in congested frequency bands, ensuring reliable communication. With its elastic conductive fabric, the MKKTN260-based antenna enhances comfort and versatility, promising to redefine wearable communication devices and elevate user experience [6].

The rollout of 5G wireless networks utilizing frequencies between 4.8 and 5.0 GHz necessitates the development of compact MIMO antenna systems, such as 4x4, 8x8, and 10x10 topologies, integrating co-located self-neutralized loop and monopole antenna pairs. Remarkably small with dimensions of $6.7\times15.5\times3.08$ mm³, these antenna systems meet contemporary communication device space requirements while delivering significant performance enhancements. This high degree of isolation is critical for reducing interference and enhancing data transmission reliability in MIMO systems. Moreover, the novel design achieves a remarkable 50% size reduction compared to traditional antenna arrangements, enhancing overall efficiency and miniaturization of 5G-capable equipment [7]. Originally intended for a 1x2 MIMO configuration, a ground-breaking huge MIMO antenna decoupling structure addresses mutual coupling issues between closely spaced dipoles. Through the clever use of C-shaped and end-folded metal strips, this construction achieves a remarkable 5 dB reduction in mutual coupling, enhancing isolation between neighboring antenna elements. The thoughtful positioning of metal strips establishes this structure as a pioneering approach to enhancing communication systems in the rapidly evolving field of next -generation wireless technology [8]. Designed for 5G devices, a 10-port hybrid MIMO antenna system combining single- band and multi-band modules achieves excellent isolation between antenna elements in both modules, with reflection coefficients below -6 dB and -10 d B for multi-band and single-band modules, respectively [9].

A new Super Wide Band (SW B) antenna, designed on a flexible Ultralow 3850 substrate (60 x 40 x 0.1 mm³), is introduced in this study, boasting a remarkable bandwidth ratio of 57.47:1 and operating between 1.74 and 100 GHz. With applications spanning across 5G and IoT, this antenna offers versatility across a wide range of wireless applications. Experimental validation using a programmable network analyzer and simulation analysis covering reflection coefficient, radiation pattern, gain, efficiency, and surface current confirm its performance [10]. In another endeavor, a low-power CMOS impulse ultra-wideband transceiver system architecture is proposed, aiming for an impressive 1mW power consumption. Tailored for sensor network applications with modest data

rates and short communication ranges, the transceiver employs a primarily digital architecture, strategically placing the A/D converter near the antenna and utilizing basic digital switches for pulse creation within the lower FCC UWB band. The digital backend is streamlined, featuring a pulse template correlation filter block and additional spreading code to optimize power efficiency and conserve space [11]. Meanwhile, addressing challenges in high-data-rate pulsed ultra-wideband systems, a modular platform for designing prototypes and developing system specifications is presented. This prototype incorporates wideband direct conversion front-end, UWB antennas for wireless communication, and binary phase shift keyed pulses for data modulation, with considerations for customized chipsets based on insights gained from discrete prototypes, targeting operation in the 3.1–10.6 GHz range [12]. For indoor positioning systems, a circularly polarized (CP) RFID reader antenna with dual ports and dual bands is designed to function in the lower ultra-wideband (UWB) and ultrahigh frequency (UHF) bands. This antenna achieves high gain, wide bandwidth, and CP operation in a low-profile design by employing a shared aperture with a hybrid mode concept and a quadruple feed network. In the UHF spectrum, it demonstrates a minimum in-band gain of 9 dB and a measured 3-dB axis ratio (AR) spectrum spanning 0.918 to 0.926 GHz. It displays a measured 3-dB AR bandwidth and a 10-dB impedance bandwidth from 3 to 5.2 GHz for the lower UWB band (3.1-4.8 GHz), with a minimum in-band gain of 9 dB. In the neighborhood of the 2.45 and 5.8 GHz wireless local area network frequencies, gain suppression exceeds 20 dB [13]. Meanwhile, the production of ultra-wideband (UWB) pulses presents challenges due to the necessity for high voltages (>500 kV) and rapid rising times (≈100 ps). Research by the Air Force Research Laboratory (AFRL) explores precision switching of high voltages using gas and oil media, alongside investigations into solid-state and oil switch technologies. These developments in UWB transmitters and high-voltage switching hold promise for applications in communications, target identification, and transient radar [14]. Furthermore, cognitive radios rely on secondary devices to detect primary user presence for utilizing underutilized spectrum. Examining UWB device detection and avoidance strategies in WiMAX bands, challenges in implementing fundamental detection and avoidance capabilities robustly on-chip are discussed. Measurement findings underscore potential interference issues and the challenge of resolving listen-before-speak primaries in coexistence scenarios [15]. A wearable antenna with a low-profile design that uses metamaterial is proposed for wireless applications. It is 4.2 mm thick, textile-based, and operates between 3 and 11 GHz. With the use of metamaterial structure, HFSS software analysis shows improved gain and directionality, which lowers Specific Absorption Rate (SAR) values for efficient use in WBAN and Ultra-wide Band applications [16-21].

2 Antenna Design

The Rogger5880 dielectric substrate of relative permittivity is used in the construction of the suggested antenna (εr) of 2.2. Due to the flexibility and accuracy of the Rogers, it is used as substrate. The antenna's overall dimensions is $20 \times 15 \times 0.5$ mm3.The patch of the microstrip antenna is first designed as rectangular shape and later bend into the obtained structure to resonant at the required

Parameters	Value	Parameters	Value
Ls	20.0	**d_2**	6.50
Ws	15.0	**Lp**	4.53
Wp	0.88	**L_1**	3.50
Lg	12.5	**L_2**	4.90
Wg	11.5	**g**	0.50
d_1	4.85		

Table 1: **Dimension of the proposed antenna**

frequency. The purpose of the flawed ground structure is to enhance impedance matching of the antenna. The fig.1 shows the proposed patch view and ground view of the antenna. The dimensions of the antenna are shown in table 1. By adjusting the width of the monopole in the ground plane the bandwidth can be increased and at a particular width, the maximum bandwidth can be obtained. This antenna is designed and simulated in the CST software

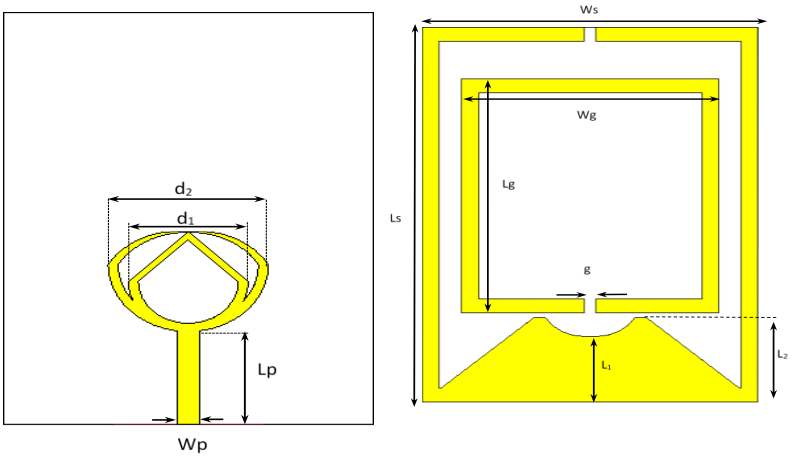

.**Figure 1**: Patch view and ground view of the antenna

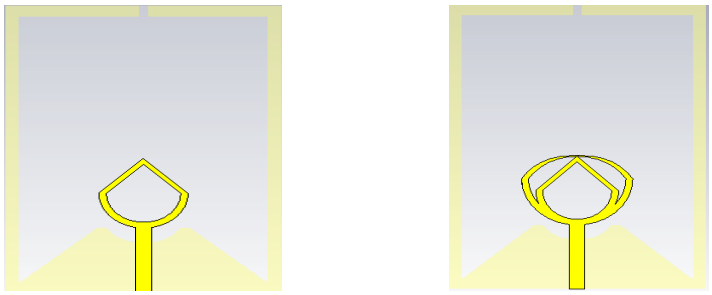

(a) (b)

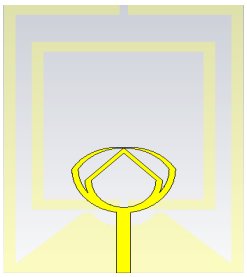

(c)

Figure.2: (a) stage I: microstrip line-fed ring-based resonator with triangular cuts on either end in the partial ground plane; (b) stage II: concentric ring added to the patch; and (c) stage III: monopoles added to the ground plane.

In the stage 1 the ground plane is designed but cutting the two edges of the partial ground into triangular shape and small cut is made at the centre of the partial ground as in fig.2(a). The patch was blended to from as circle at the bottom and triangular at the top. This shape of the antenna made to resonant at the higher frequencies and the ground plane that is utilized to match impedances.

In the stage 2 the concentric ring was added to the patch as shown in fig.2(b) to make it resonant at wide range of frequency. For supporting the impedance matching to the modified antenna the monopole is added to the ground plane in the stage 3 as in fig.2(c). The width of the concentric rings is adjusted in order to resonant at the frequency of 10 – 18 GHz with a proper impedance matching.

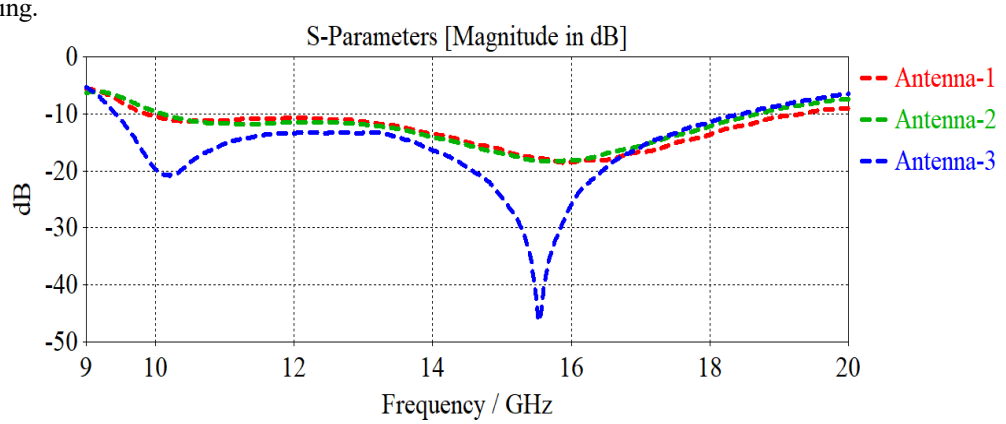

Figure.3: S-parameters of the antenna in three stages

Based on the S-parameter result obtained the antenna is design by modified the patch structure for supporting the frequency proposed and the ground for strengthening the impedance matching. The S-parameters of the antenna at three stages are represented in the fig.3. As the antenna 3 shows better results it is taken into consideration and other parameters are been tested to ensure the performance of the antenna.

3 Results & Discussion

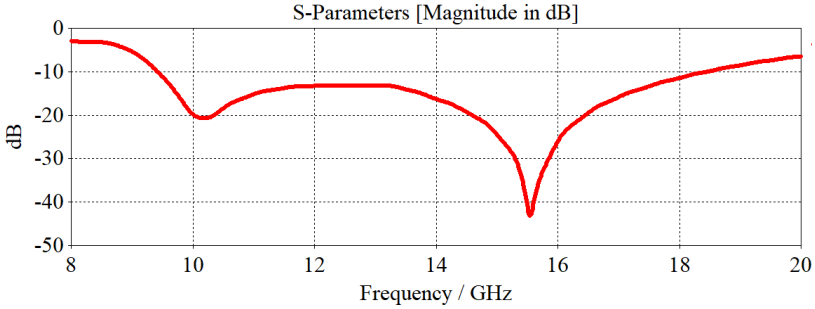

Figure.4: S-Parameter of antenna

S-parameter shows the behavior of linear electrical networks. The designed antenna is resonated at the frequency of 9.5-18.2 GHz covering a bandwidth of 8.7GHz. Fig.4 shows the reflection coefficients of the antenna when simulated. At the frequency of 15.8 GHz the S-parameter value is - 46 dB indicate good impedance matching and efficient energy transfer. For the optimal antenna performance, it is crucial to operate at low S-parameter in the specific frequency band.

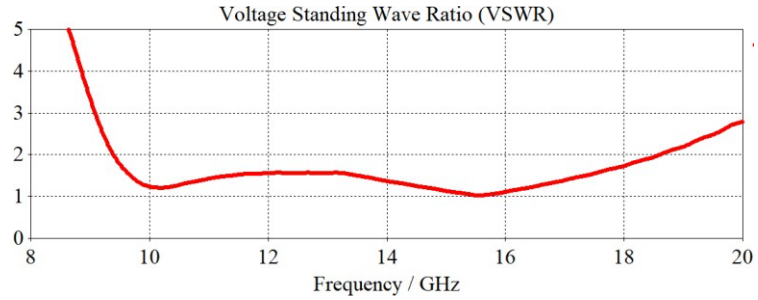

Figure.5: VSWR of the antenna

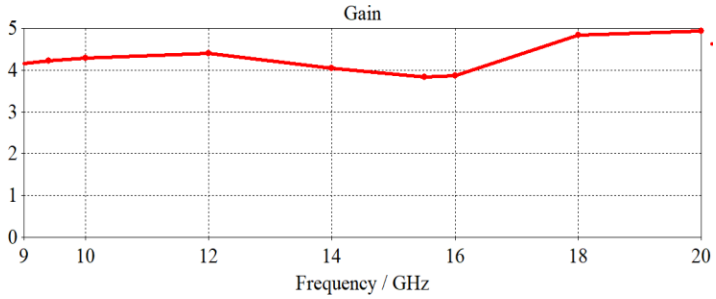

Figure.6: Gain of the antenna

VSWR provides information about how well power is transferred between the antenna and the

transmission line it is attached to it. The VSWR of designed antenna having the frequency range of 9.5 – 18.2 GHz is shown in fig.5. In this frequency range the VSWR range is between 1 to 2 indicating there are less reflections and the signal loss is minimal. In the frequency of 15.8 GHz the VSWR is 1 representing perfect impedance matching between source and load.

The antenna's gain is the fundamental characteristic used to describe how well an antenna converts input power into radiated power in a certain direction. In the specific range of frequency, the gain is between 4-5 dB shown in fig.6 indicating the efficient radiation and reception capabilities in the view of power consumption. This level of gain is valuable particularly for ultrawideband applications where high data rates are required.

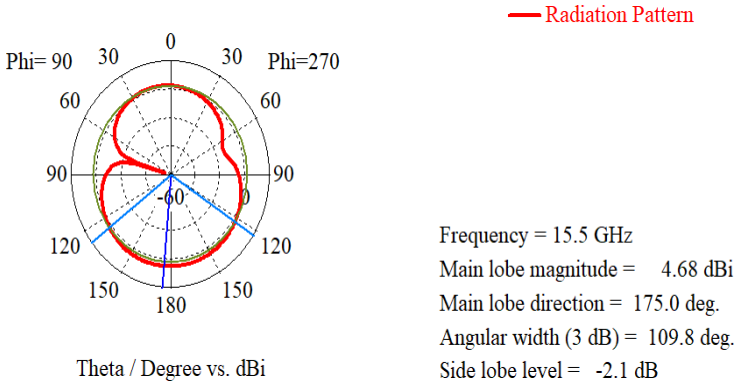

Figure.7: Radiation Pattern at 15.5 GHz

The radiation pattern at 15.5 GHz as in fig.7 reveals a prominent main lobe with the magnitude of 4.68 dB and oriented towards 175 degrees. The angular width of the main lobe spans 109.8 degrees, indicating a broad coverage area in the specified direction. Additionally, side lobes are observed with a magnitude of -2.1 dB, suggesting relatively lower radiation intensity compared to the main lobe. This configuration indicates a well-defined directional radiation pattern suitable for wireless body area network (WBAN) applications, offering robust communication coverage with minimized interference from side lobes.

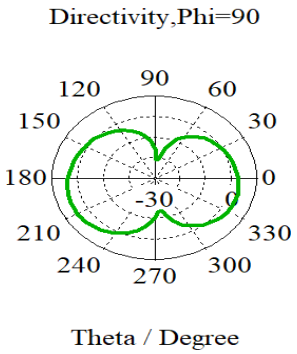

Figure.8: Directivity of the antenna

One important factor that characterizes an antenna's capacity to concentrate or direct electromagnetic energy in a particular direction is its directivity. Directivity is commonly expressed as a dimensionless ratio and is likened to the radiation properties of an isotropic radiator, a hypothetical antenna that emits radiation uniformly in all directions. A more concentrated radiation pattern, concentrating the antenna's energy in certain areas of space, is indicated by higher directivity values. Fig.8 shows the directivity of the implemented antenna. Comparison of proposed work

with existing work is shown in below Table 2.

Ref	*Frequency (GHz)*	*Substrate used*	*dimensions (mm^3)*	*Gain (dB)*	*Band Width (MHz)*
[2]	*3.5,5.8*	*FR4, ϵ_r = 4.4*	*150×75×0.8*	*2.5-5*	*800*
[3]	*2.32,5.2*	*FR4,* ϵ_r = 4.4	0.43×0.37×0.012	*9.9*	*200, 564*
[5]	*5.7-5.8*	*Felt, ϵ_r = 1.36*	*50×40×2*	*2.4-5.2*	*250*
[7]	*3.3-4.5*	*Rogers 4350B,* $\epsilon_r = 3.45$	*50×48×0.5*	*5.5-7*	*1.2 GHz*
[9]	*1.74-100*	*Ultralam 3850*	*60×40×0.1*	*1.9-10*	*98.2 GHz*
Proposed antenna	*9.5-18.2*	*Rogers 5880,* $\epsilon_r = 2.2$	*20×15×0.5*	*4-5*	*8.7 GHz*

Table 2: Comparison of proposed work with existing work

4 Conclusion

A microstrip antenna for Wireless Body Area Network (WBAN) applications, which are essential to the Internet of Things (IoT) is designed. Operating in the 9.5 to 18.2 GHz UW B frequency range, the antenna is aimed towards sports monitoring and healthcare. Strict modelling is emphasised in the design process, and cutting-edge methods like fractal geometries and compact architectures are used to minimise size without sacrificing functionality. The principal objective of the antenna is to exhibit flawless impedance matching and an all-around radiation pattern, guaranteeing dependable connectivity for body-centric Internet of Things applications in diverse sectors. This invention has the potential to improve wireless sensor networks in practical applications.

References

1. R. Liu, X. An, H. Zheng, M. Wang, Z. Gao and E. Li, "Neutralization Line Decoupling Tri-Band Multiple-Input Multiple-Output Antenna Design," in IEEE Access, vol. 8, pp. 27018-27026, 2020, doi: 10.1109/ACCESS.2020.2971038.

2. M. N. Zahid et al., "H-Shaped Eight-Element Dual-Band MIMO Antenna for Sub-6 GHz 5G Smartphone Applications," in IEEE Access, vol. 10, pp. 85619 -85629, 2022, doi: 10.1109/ACCESS.2022.3189658.

3. C. Munusami and R. Venkatesan, "A Compact Boat Shaped Dual-Band MIMO Antenna With Enhanced Isolation for 5G/WLAN Application," in IEEE Access, vol. 12, pp. 11631-11641, 2024, doi:10.1109/ACCESS.2024.3356078.

4. J. C. Dash and D. Sarkar, "Microstrip Patch Antenna System With Enhanced Inter-Port Isolation for Full- Duplex/MIMO Applications," in IEEE Access, vol. 9, pp. 156222-156228, 2021, doi:10.1109/ACCESS.2021.3128997.

5. L. Yang, Y. Xie, H. Jia, M. Qu, Z. Lu and Y. Li, "Dual- Band Flexible MIMO Antenna with Self-Isolation Enhancement Structure for Wearable Applications," in Chinese Journal of Electronics, vol. 32, no. 4, pp. 692-702, July 2023, doi: 10.23919/cje.2021.00.293.

6. C. -Z. Han, L. Xiao, Z. Chen and T. Yuan, "Co-Located Self-Neutralized Handset Antenna Pairs With Complementary Radiation Patterns for 5G MIMO Applications," in IEEE Access, vol. 8, pp. 73151-73163, 2020, doi: 10.1109/ACCESS.2020.2988072.

7. Y. Qin, R. Li and Y. Cui, "Embeddable Structure for Reducing Mutual Coupling in Massive MIMO Antennas," in IEEE Access, vol. 8, pp. 195102-195112, 2020, doi: 10.1109/ACCESS.2020.3033717.

8. R. Ullah, S. Ullah, R. Ullah, F. Faisal, I. B. Mabrouk and M. J. A. Hasan, "A 10-Ports MIMO Antenna System for 5G Smart-Phone Applications," in IEEE Access, vol. 8, pp. 218477-218488, 2020, doi: 10.1109/ACCESS.2020.3042750.

9. S. Dey, M. S. Arefin and N. C. Karmakar, "Design and Experimental Analysis of a Novel Compact and Flexible Super Wide Band Antenna for 5G," in IEEE Access, vol. 9, pp. 46698-46708, 2021, doi: 10.1109/ACCESS.2021.3068082.

10. U. Pandey, P. Singh ,R. Singh ,N.P. Gupta , S.K. Arora ,and E. Nizeyimana ,"Miniaturized Ultrawideband Microstrip Antenna for IoT-Based Wireless Body Area Network Applications" , Wireless Communications and Mobile Computing, 2023.

11. D. O'Donnell and R. W. Brodersen, "An ultra-wideband transceiver architecture for low power, low rate, wireless systems," in IEEE Transactions on Vehicular Technology, vol. 54, no. 5, pp. 1623-1631, Sept. 2005, doi: 10.1109/TVT.2005.854021.

12. D. D. Wentzloff, R. Blazquez, F. S. Lee, B. P. Ginsburg, J. Powell and A. P. Chandrakasan, "System design considerations for ultra -wideband communication," in IEEE Communications Magazine, vol. 43, no. 8, pp. 114-121, Aug. 2005, doi: 10.1109/MCOM.2005.1497561.

13. J. Zhang and Z. Shen, "Dual-Band Shared-Aperture UHF/UW B RFID Reader Antenna of Circular Polarization," in IEEE Transactions on Antennas and Propagation, vol. 66, no. 8, pp. 3886-3893, Aug. 2018, doi: 10.1109/TAP.2018.2839883.

14. F.J. Agee et al., " Ultra-wideband transmitter research," in IEEE Transactions on Plasma Science, vol. 26, no. 3, pp. 860-873, June 1998, doi: 10.1109/27.700855.

15. S. M. Mishra, R. W. Brodersen, S. t. Brink and R. Mahadevappa, "Detect and avoid: an ultra-wideband/WiMAX coexistence mechanis m [Topics in Radio Communications]," in IEEE Communications Magazine, vol. 45, no. 6, pp. 68-75, June 2007, doi: 10.1109/MCOM.2007.374435.

16. B.Alekya, N. A. Murugan and B. T. Phani Madhav, "Analysis of Wearable Antenna using metamaterial for wideband Applications," 2022 International Conference on Power, Energy, Control and Transmission Systems (ICPECTS), Chennai, India, 2022, pp. 1-5, doi: 10.1109/ICPECTS56089.2022.10047257.